European Polymer Journal 197 (2023) 112377

Contents lists available at ScienceDirect

European Polymer Journal

journal homepage: www.elsevier.com/locate/europolj

In vivo and *in vitro* biocompatible alginate film crosslinked with Ca^{2+} and Co^{2+} manifests antiviral, antibacterial and anticancer activity

Alba Cano-Vicent [a], Andrea Martínez-Agut [a], Alberto Tuñón-Molina [a], Hamid Bakshi [b], Roser Sabater i Serra [c,d,e], Iman M. Alfagih [f], Murtaza M. Tambuwala [g,*], Ángel Serrano-Aroca [a,*]

[a] *Biomaterials and Bioengineering Lab, Centro de Investigación Traslacional San Alberto Magno, Universidad Católica de Valencia San Vicente Mártir, 46001 Valencia, Spain*
[b] *Hormel Institute, University of Minnesota, Austin, MN 55912, United States*
[c] *Centre for Biomaterials and Tissue Engineering, Universitat Politècnica de València, València 46022, Spain*
[d] *Biomedical Research Networking Centre in Bioengineering, Biomaterials and Nanomedicine (CIBER-BBN), València 46022, Spain*
[e] *Department of Electrical Engineering, Universitat Politécnica de Valencia, Valencia 46022, Spain*
[f] *Department of Pharmaceutics, College of Pharmacy, King Saud University, Riyadh, ZIP 4545, Saudi Arabia*
[g] *Lincoln Medical School, University of Lincoln, Brayford Pool Campus, Lincoln LN6 7TS, United Kingdom*

ARTICLE INFO

Keywords:
Alginate
Cobalt
Toxicity
Antiviral
Antibacterial
Anticancer

ABSTRACT

Alginate crosslinked with calcium cations is a promising hydrogel for biomedical applications as it is non-toxic, has suitable mechanical properties and is insoluble in water. Cobalt has been shown to possess antibacterial capacity against Gram-positive and Gram-negative bacteria, and has an angiogenesis effect. In this study, alginate films were crosslinked with Ca^{2+} and Co^{2+} ions to explore their biological properties in terms of antiviral capacity, antibacterial properties, anticancer activity and their toxicity. The results show that the hydrogel with a very small amount of cobalt was biocompatible *in vivo* using the *Caenorhabditis elegans* model and *in vitro* on human keratinocyte cells and it also exhibited antibacterial activity against the life-threatening methicillin-resistant *Staphylococcus aureus*. Furthermore, this hydrogel showed antiviral activity against a surrogate of SARS-CoV-2 and anticancer properties against melanoma and colon cancer cells, which render it a promising material for biomedical applications such as wound healing and tissue engineering. Water sorption experiments, Fourier transform infrared spectroscopy, electron microscopy with Energy Dispersive X-ray Spectrometry and degradation analysis in acid aqueous medium were performed to complete the characterization of these new materials.

1. Introduction

Hydrogels are three-dimensional crosslinked polymeric structures which can absorb large amounts of water, due to the hydrophilic groups of their polymeric skeleton. They also have high strength, good flexibility and are insoluble in water [1]. Alginate is a promising biopolymer among the most common hydrogels for potential use in biomedical applications [2] and is obtained mainly from brown algae (*Laminaria* sp. and *Fus vesiculosus*). They are linear polymers formed by alternating guluronic (α-L-guluronic) and mannuronic (β-D-mannuronic) acid units, polyguluronic zones and polymannuronic zones [3]. This hydrogel has a large number of industrial and biomedical applications such as water treatment, tissue engineering and drug delivery [4].

No toxicity of alginate hydrogels has been observed in either *in vitro* or *in vivo* assays [5,6]. Their biological properties can be enhanced by adding other compounds with intrinsic antimicrobial properties such as silver, zinc, cobalt, copper or carbon-based materials [7,8]. Alginate crosslinked with bacterial cellulose and cobalt hydrogel thus showed antibacterial activity against *E. coli* and *S. aureus* [9]. Alginate-based hydrogels are promising as a drug delivery system to treat cancer cells,[10–12] while alginate crosslinked with a cobalt matrix incorporating selenium-modified borosilicate glass showed angiogenesis and anti-microbial effects [13]. Alginate dopamine hydrogel loaded with an anticancer drug improved cytotoxicity against squamous cancer and colon cells [14]. In this study, alginate hydrogel films were prepared by solvent casting and subsequent crosslinking with Ca^{2+} and different amounts of Co^{2+} for the first time. Our aim was to study the biological properties of these novel hydrophilic films in terms of toxicity, both *in*

* Corresponding authors.
E-mail addresses: MTambuwala@lincoln.ac.uk (M.M. Tambuwala), angel.serrano@ucv.es (Á. Serrano-Aroca).

https://doi.org/10.1016/j.eurpolymj.2023.112377
Received 1 February 2023; Received in revised form 1 August 2023; Accepted 20 August 2023
Available online 22 August 2023

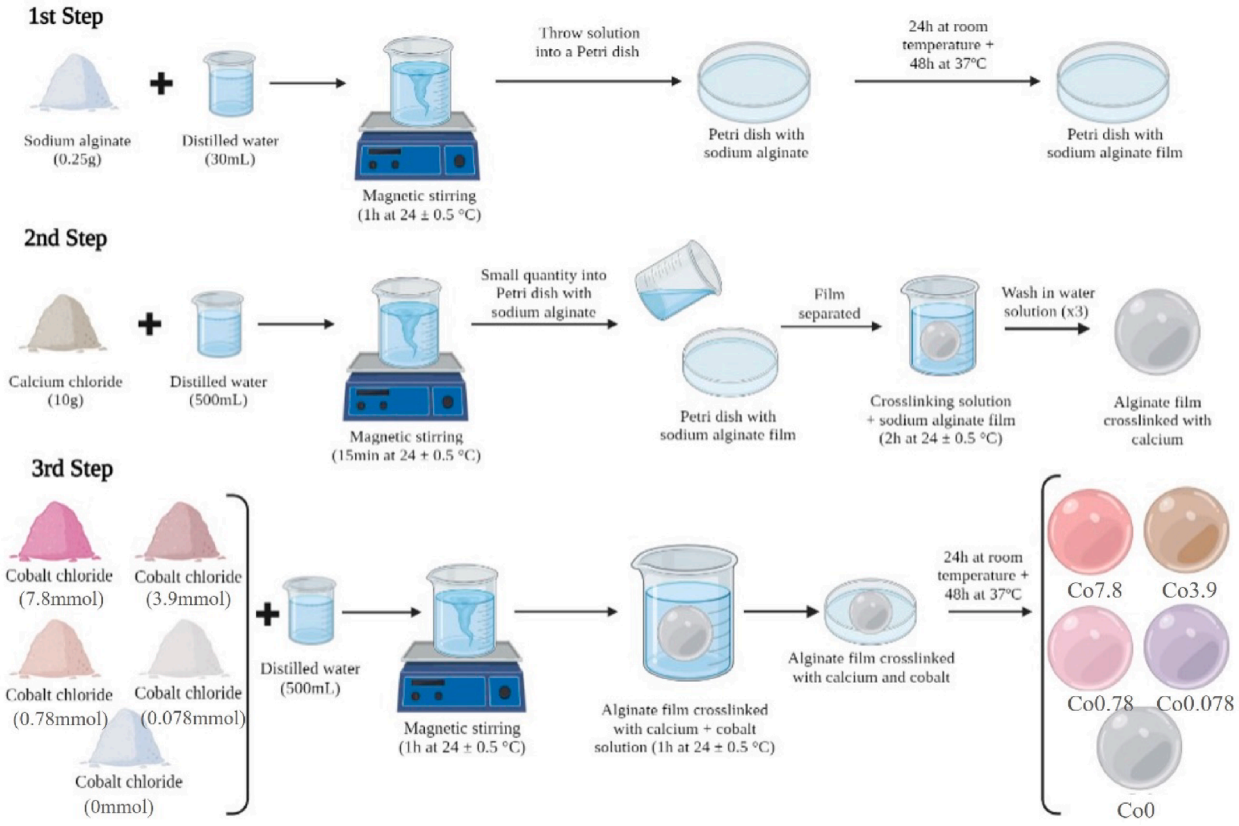

Fig. 1. Schematic of the film preparation.

vitro and *in vivo* and their antiviral, antibacterial and anticancer properties.

2. Materials and methods

2.1. Materials

Sodium alginate, calcium chloride (≥93.0%) and cobalt (II) chloride (≥98.0%) were purchased from Sigma-Aldrich (Saint Louis, MO, USA). The alginate used had previously been characterized [3] and showed a fraction of guluronic (G) blocks of 0.463, a fraction of mannuronic (M) blocks of 0.537, or M/G ratio of 1.16, a fraction of GG blocks of 0.282, a fraction of MG blocks of 0.181, a fraction of MM blocks of 0.356, a fraction of GGM blocks and MGG blocks of 0.048, and a fraction of GGG blocks of 0.234. The guluronic acid blocks were mostly arranged in short G-blocks (average length ~ 7). Fetal bovine serum (FBS), DMEM low glucose, penicillin–streptomycin (P/S), L-glutamine and Epidermal Growth Factor (EGF) were obtained from Life Technologies (Gibco, Karlsruhe, Germany). Bacteriological agar from Scharlau (Ferrosa, Barcelona, Spain). Typtic soy broth (TSB) and typtic soy agar (TSA) from Liofilchem.

2.2. Synthesis

0.25 g of sodium alginate was dissolved in 30 mL of distilled water and dispersed by magnetic stirring for 1 h at 24 ± 0.5 °C. This solution was put into a Petri dish and left for 24 h at room temperature, followed by 48 at 37 °C. The crosslinking solution was prepared by dissolving 10 g of calcium chloride in 500 mL of distilled water and dispersed by magnetic stirring for 15 min at 24 ± 0.5 °C. A small quantity of this solution was then placed in the Petri dish with sodium alginate. When the film separated, it was put into the crosslinking solution for 2 h at 24 ± 0.5 °C. After that, the film was washed three times in a water solution to remove any residual crosslinker. Subsequently, different quantities of cobalt chloride (0, 7.8, 3.9, 0.78 and 0.078 mmol) were diluted in 500 mL of distilled water. The film was placed in its corresponding cobalt

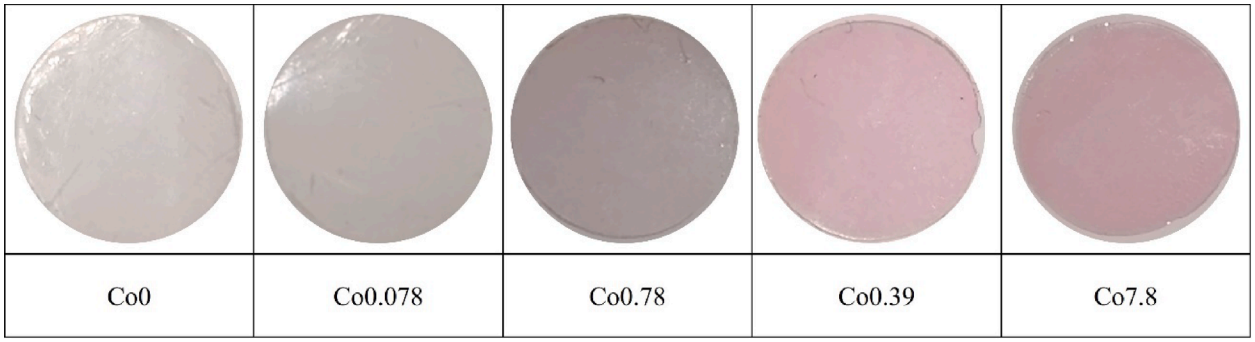

Fig. 2. Alginate films crosslinked with calcium and cobalt cations.

chloride solution for 1 h at 24 ± 0.5 °C. It was then poured into a Petri dish and left for 24 h at room temperature, followed by 48 at 37 °C in an oven. These samples are hereinafter referred to as Co7.8, Co3.9, Co0.78, Co0.078 and Co0 films, according to the number of cobalt chloride grams used in the synthetic procedure (Fig. 1).

Fig. 2 shows how the hydrogel films take on a pinkish color with increasing cobalt content. Disks 10 mm in diameter were obtained from the hydrogels with a cylindrical punch. The samples were then subjected to ultraviolet radiation for 1 h per side for sterilization.

2.3. Swelling ratio

The films were dried at 60 °C for 48 h to constant weight, after which they were weighed and placed in 100 mL of distilled water and left in an oven at 37 °C. Thus, they were weighted at different water sorption times (30 min, 5 h, and 24 h). The water sorption (h) was calculated by the following Eq. (1):

$$h = \left(\frac{m_{hydratedfilm} - m_{dryfilm}}{m_{dryfilm}} \right) \quad (1)$$

where $m_{hydrated\ film}$ is the weight of the swollen film for each time and $m_{dry\ film}$ is the weight of the dry film.

2.4. Electron microscopy.

The composition of the hydrogels was analyzed by field emission scanning electron microscope (FESEM) (Zeiss ULTRA 55, Carl Zeiss Microscopy) with Energy Dispersive X-ray Spectrometry (EDX, X-Max N, Oxford Instruments). The samples were coated with a carbon layer using a sputter coating (EM MED020, Leica). The percentages of Ca and Co ions were obtained with the EDX in three different zones of the surface at an accelerating voltage of 15 kV.

2.5. Fourier transform infrared spectroscopy (FTIR)

FTIR (Bruker ALPHA II Compact FT-IR Spectrometer) was used to study the surface functional groups in a transmittance mode. All spectra were scanned at room temperature over the wave number range of 4000——400 cm − 1 using 30 scans at a resolution of 2 cm^{-1}.

2.6. Degradation analysis

The quantitative results of this study were based on the weight control of the films for 3 months in an acid aqueous degradation medium (pH 6). The acid aqueous medium was composed of deionized water with a pH adjusted to 6 with a 10% HCl solution in water. Initially, the materials were vacuum dried at 60 °C to determine the dry mass of each material. Samples were introduced into 50 mL falcon tubes containing the degradation medium (40 mL per flask) and placed in the shaking bath with a shaking frequency of 80 r.p.m. at 37 °C. The experimental degradation times were 1, 2 and 3 months. Three replicates of each material per time were analyzed to provide reproducible results. After each selected degradation time, the materials were extracted and dried to constant weight to determine the weight loss and morphological changes.

2.7. Toxicological in vitro study

All the 10 mm diameter disks were placed in a 6-well plate with DMEM (Biowest SAS, France) FBS, a volume ratio of 3 cm^2/mL was selected, in accordance with ISO-10993, which recommends this rate for tube wall, slab and small molded articles.

The biomaterials were incubated in humidified 5% CO_2/95% ambient air for 72 h at 37 °C. A cell line of non-tumorigenic immortalized human keratinocyte HaCaT cells was provided from the Medical Research Institute Hospital La Fe, Valencia, Spain. Cell incubation was carried out in a mixture of DMEM with 10% FBS, 1% w/v penicillin (Lonza, Belgium), and 1% w/v streptomycin (HyClone, GE Healthcare Life Sciences), at 37 °C and 5% CO_2. The MTT assay was used to measure the effect of the hydrogel treatment on cell viability The HaCaT cells were planted at 10^4 cells/well on a 96-well plate and incubated for 24 h at 37 °C, after which the medium in each well was replaced by 100 μL of hydrogel extracts. The medium was also replaced by 100 μL of the same medium used to produce the hydrogel extracts (positive control) as well as 100 μL of 1000 μM zinc chloride (≥97.0%, Sigma-Aldrich) solution as negative control, as this concentration is highly toxic to HaCaT cells [15]. Cell incubation was carried out with 5 mg/mL MTT in each well for 3 h. 100 μL dimethyl sulfoxide (Sigma-Aldrich) was added at ambient temperature and the absorbance was read at 550 nm on a microplate reader (Varioskan, Thermo Fisher).

2.8. In vivo toxicity tests

In vivo toxicity was studied in the *Caenorhabditis elegans* model. Extractions from the Co7.8, Co3.9, Co0.78, Co0.078 and Co0 Co7.8Co3.9Co0.78Co0.078films were accomplished following the ISO-10993 standard recommendations. Potassium medium (2.36 g potassium chloride, 3 g sodium chloride in 1 L distilled water, autoclaved) was added from each well of a 6-well plate in accordance with ISO-10993. After incubating for 72 h at 25 °C, extracts were collected in 1.5 mL Eppendorf tubes.

The N2 strain used in these experiments was provided by the *Caenorhabditis* Genetics Center (CGC, Minneapolis, MN, USA). The worms were maintained and propagated on OP50 *E. coli* seeded nematode growth medium (NGM) at 25 °C. The NGM plates were washed with 5 mL of distilled water to collect the worms in 15 mL falcon tubes.

The NGM plates were washed with 5 mL of distilled water to collect the worms in 15 mL falcon tubes. The *C. elegans* were synchronized, for which the tubes were centrifuged at 1300 r.p.m. for 3 min. The pellet containing the worms was resuspended in 100 μL of distilled water. 700 μL of a 5% bleaching solution was added to this resuspension. This mixture was vortexed every 2 min for 15 min, after which the tubes were centrifuged at 700x g for 3 min. The pellet with the worm eggs was washed in 800 μL of distilled water and this step was repeated twice. Finally, the pellet was resuspended in 100 μL of distilled water and transferred to NGM plates seeded with 100 μL of an OP50 *E. coli* culture. The plates were incubated for 72 h at 25 °C and washed with distilled water. The wash was centrifuged to collect the L1-stage worm population. The pellet was resuspended in 3 mL of potassium medium 62.5 μL of a 1:250 suspension of cholesterol (5 mg/mL in ethyl alcohol) in a sterile potassium medium, 62.5 μL of a 50x concentrated OP50 *E. coli* culture. 115 μL of potassium medium and 250 μL of the pertinent extract were added to a each well of a 48-well plate and a volume of K medium containing 50–100 worms was added. The plates were sealed with parafilm and placed in an orbital shaker at 25 °C and 120 r.p.m. for 24 and 72 h. The positive control was worms incubated with a medium only and without extracts. The negative control was worms incubated with a zinc dilution. For the survival rate of *C. elegans,* the number of living and dead worms were counted. The mixture incubation with the extracts and the worms was divided into 10 drops of 50 μL and placed under a microscope (Motic BA410E including Moticam 580 5.0MP). To analyze reproduction, three worms were placed on a new OP50 seeded NGM plate and allowed to lay eggs for 48 h. The eggs were then counted under the microscope. Body lengths were measured in a photo taken under the microscope by Motic Images Plus 3.0 software. Five independent replicates (n = 5) were conducted.

2.9. Antibacterial activity

The hydrogels were put into a tube with a dilution of methicillin-resistant *Staphylococcus aureus*, COL [16] in a concentration of about

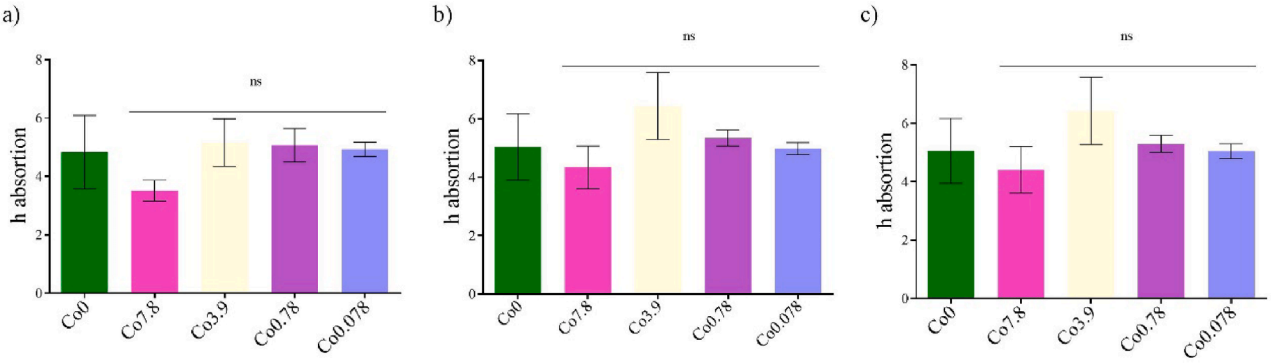

Fig. 3. Water absorption (($m_{hydrated\ film} - m_{dry\ film}$)/$m_{dry\ film}$) of the calcium alginate film (Co0) and films crosslinked with different amounts of cobalt (Co7.8, Co3.9, Co0.78 and Co0.078) after 30 min (a), 5 h (b) and 24 h (c) at 37 °C. The results of the statistical analysis between the untreated film (Co0) and the films crosslinked with different amounts of cobalt are shown: ns: not significant.

1×10^6 CFU/mL in TSB. A volume ratio of 3 cm^2/mL was selected, following ISO-10993 and placed in an orbital shaker at 37 °C and 240 r.p.m. for different study times (24 h and 15 h). The falcon tubes were then vortexed for 1 min and serial dilutions were taken from each sample. 100 μL of each dilution was added to the TSA plate and was extended with a spreader. The plates were incubated for 18–24 h in an oven at 37 °C. The number of colonies in CFU/mL in each sample were compared with the control, which consisted of a falcon tube with only bacteria without a sample. Three independent antibacterial tests were made on two different days (n = 6) to guarantee reproducibility.

2.10. Anticancer study

The 10 mm-diameter disks were placed in a tube with DMEM (Biowest SAS, France) without FBS, covering the whole surface area. The ISO-10993 standard, which recommends a volume ratio of 3 cm^2/mL for irregular low-density porous materials were followed.

The biomaterials were incubated in humidified 5% CO_2/95% ambient air for 72 h at 37 °C. A colon cancer cell line (HT-29) and melanoma (B16) [17–19]. were used. Cell incubation was performed in a mixture of DMEM with 10% FBS, 1% L-glutamine and 1% penicillin/streptomycin (Thermo Scientific Hyclone, Logan, UT, USA) at 37 °C and 5% CO_2. The MTS assay was used to measure the effect of the treatment with the hydrogels. The cells were planted in a 96-well plate at $1x10^5$ cells/well and incubated for 24 h at 37 °C. The medium in the wells was replaced with 100 μL of hydrogel extracts. Three serial dilutions of each extract were made. The medium was also replaced with 100 μL of the medium used to produce the hydrogel extracts (control). The cell with the hydrogel extract was incubated in humidified 5% CO_2/95% ambient air for 24 h at 37 °C. The MTS solution (20 μL) was added to each cell culture well, the plate was incubated at 37 °C for 4 h and then analyzed at 490 nm (Flurostar Omega plate reader, BMG Labtech, Aylesbury, UK).

2.11. Antiviral test using enveloped bacteriophage Φ6

The Gram-negative *Pseudomonas syringae* (DSM 21482) from the Leibniz Institute DSMZ-German Collection of Microorganisms and Cell Cultures GmbH (Braunschweig, Germany) was grown on a TSA plate and after in liquid TSB at 25 °C at a speed of 120 rpm. The enveloped bacteriophage Φ6 (DSM 21518) was propagated following the specifications provided by the Leibniz Institute.

50 μL of a bacteriophage suspension, at a titer of approximately 1×10^6 PFU/mL, in TSB was added to each disk and incubated for 24 h. The bacteriophage suspension was added to each disk from a falcon tube with 10 mL TSA. The tubes were sonicated for 5 min at 25 °C and subsequently vortexed for 1 min. Serial dilutions were made for each sample. 100 μL of the host strain at $OD_{600nm} = 0.5$ was mixed with 100 μL of each bacteriophage dilution. The infective activity of the bacteriophage was determined by the double-layer method [20]. The bacteriophage-bacteria suspension was mixed with 4 mL of top agar (TSB + 0.75% bacteriological agar) with 1 mM $CaCl_2$ to be finally poured onto TSA plates. The plates were incubated at 25 °C for 24 h. The bacteriophage titer of each sample was calculated and expressed in PFU/m for comparison with the control. The control consisted of the bacteriophage-bacteria suspension not in contact with any disk. The control will also ensure that the sonication/vortexing treatment does not affect the bacteriophage's infectious activity. The antiviral tests were performed in triplicate on two different days (n = 6) to guarantee reproducible results.

Table 1
EDX analysis of alginate hydrogels crosslinked with calcium and different amounts of cobalt.

Muestra	Ca (wt%)	Co(%wt)
Co0	13.79 ± 0.59	0
Co0.078	11.34 ± 0.34	0.28 ± 0.02
Co0.78	9.86 ± 0.42	4.26 ± 0.28
Co3.9	4.78 ± 0.16	10.00 ± 0.17
Co7.8	1.98 ± 0.05	13.80 ± 0.33

2.12. Statistical analysis

The student's *t*-test was performed for pair comparisons and one-way analysis of variance for multiple value comparisons, followed by Tukey's post hoc test (*p > 0.05, ***p > 0.001) on GraphPad Prism 6 software.

3. Results and discussion

3.1. Swelling ratio

The films were weighed at 3 different times (30 min, 5 h and 24 h) at 37 °C to calculate the absorption h, defined as the mass of water divided by the mass of the dry film (Fig. 3).

The absorption h of liquid water at 37 °C did not show statistically significant differences between the Co0 film and the cobalt films (Co7.8, Co3.9, Co0.78 and Co0.078) after 30 min, 5 h and 24 h. Therefore, all these hydrophilic films present similar water absorption capacity.

3.2. Electron microscopy

To confirm the presence of Ca and Co ions, the cross-linked hydrogels were analyzed by EDX (Table 1).

Although the EDX technique is semiquantitative, the results indicate the presence of Ca^{2+} and Co^{2+} in the samples Co0.078, Co0.78, Co3.9 and Co7.8. The concentration of Co^{2+} ions increases with increasing the

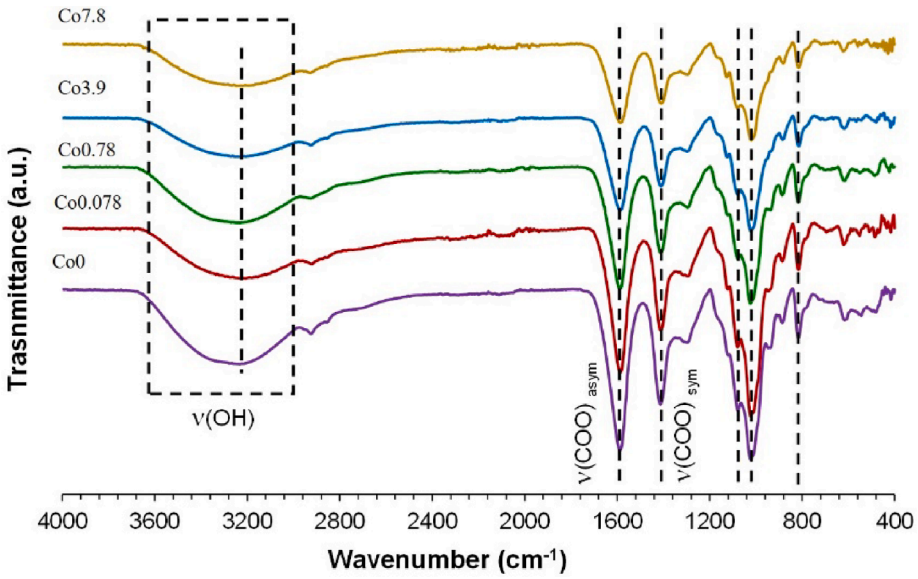

Fig. 4. FTIR spectra in the 4000–300 cm^{-1} region of the alginate hydrogel films (Co0, Co0.078, Co0.78, Co3.9 and Co7.8).

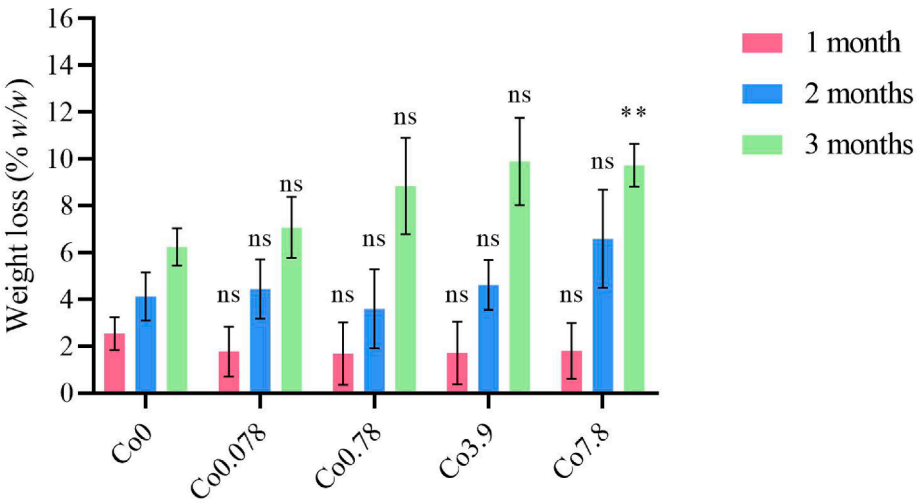

Fig. 5. Weight loss of the untreated film (Co0) and film treated with different amounts of cobalt (Co7.8, Co3.9, Co0.78, Co0.078) after degradation in acid aqueous medium (pH = 6) for 1, 2 and 3 months. Data are shown as mean ± standard deviation. The results of the statistical analysis between the untreated film (Co0) and the films crosslinked with different amounts of cobalt are shown: **p > 0.01; ns: not significant.

amount of cobalt chloride used in the film preparation, However, the percentage of Ca^{2+} ions decreases with increases the amount of Co^{2+} ions probably due to ion exchange.

3.3. Fourier transform infrared spectroscopy (FTIR)

The FTIR spectra of the different hydrogels are shown in Fig. 4. The spectrum of the calcium alginate hydrogel (Co0) presents the characteristic peaks at 822 cm^{-1} related to CH flexure, 1012 cm^{-1} related to CCH flexure, and COH, and 1047 cm^{-1} associated with the CO and CCC stretching. The peaks at 1414 and 1587 cm^{-1} can be attributed to the stretching vibration of the COO carboxylate groups (symmetric and asymmetric, respectively) and the broad peak between 2900 and 3600 cm-1 is related to the OH stretching vibration [21,22]. As expected, Ca^{2+} and Co^{2+} cross-linked alginate hydrogels show peak location in similar positions, because binding of Ca and Co ions to alginate is similar, as previously reported [23]. Ca and Co cations bind preferentially to the G blocks of the alginate, giving rise to the egg-crate structure [24].

3.4. Degradation analysis

The results of weight loss after the degradation assay in the acid aqueous medium are shown in Fig. 5.

The results confirm that higher concentration of Co^{2+} ions caused a higher degradation of the alginate-based hydrogel. The untreated film (Co0) shows a weight loss of 6% after 3 months in acid aqueous medium. Nevertheless, the weight loss of the Co7.8 film was 10% after 3 months in acid aqueous medium.

Therefore, these new hydrogels containing cobalt are quite stable in acid aqueous medium with a weight loss of only 10 % *w/w* after 3 months, which could be very interesting for certain biomedical applications.

3.5. In vitro toxicological study

The results of the toxicity assays of the hydrogel extracts in the presence of human keratinocyte HaCaT cells are shown in Fig. 6.

Extracts of Co0 and Co0.078 samples showed no statistically

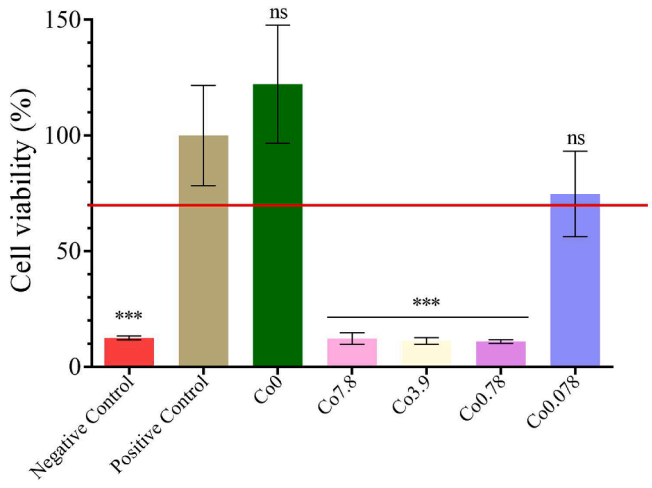

Fig. 6. 3-[4,5-dimethylthiazol-2-yl]-2,5-diphenyl tetrazolium bromide (MTT) cytotoxicity test of extracts acquired from untreated film (Co0), film treated with different weights of cobalt (Co7.8, Co3.9, Co0.78, Co0.078Co7.8Co3.9-Co0.78Co0.078), positive and negative controls cultured with human keratinocyte HaCaT cells at 37 °C. ***p > 0.001; ns: not significant.

significant differences in cell viability (%) to those of the positive control, although Co7.8, Co3.9 and Co0.78 showed statistically significant reductions in cell viability (%). The film without cobalt ions (Co0) and the Co0.078 film are therefore biocompatible in the presence of human keratinocyte cells.

3.6. *In vivo toxicity assay*

The characteristics of the *Caenorhabditis elegans* model make it an ideal living system for the analysis of its survival against exposure to specific materials or particles. Toxicity classification in *C. elegans* has been shown to be as predictively reliable as rat or mouse LD50 [25]. It also possesses human proteins, lipids, genes, and signaling methods, and its digestive system is similar in many aspects to those of mammals [26–30]. The genomics of this nematode is used to study human development and disease [26] and it involves few ethical problems. In many cases their conserved toxic action mechanisms have been found to be similar to those of mammals, apart from the fact that it has genes for most of the molecular components of the vertebrate brain. These consistent correlations make it possible to include trials using this model for early safety-testing and as an integrated or staggered toxicity testing strategy, thus allowing an intermediate stage between *in vivo* and clinical trials [31]. The worms' different parameters were analyzed after a 24 h exposure 24 h (acute toxicity) to the cobalt extracts for survival rate (Fig. 7a), reproduction (Fig. 7b) and body length (Fig. 7c), and after a 72 h exposure (chronic toxicity) for survival rate (Fig. 7d), reproduction (Fig. 7e) and body length (Fig. 7f).

The extract of the cobalt films after 24 h of exposure (acute toxicity) showed no significant difference with the positive control (Fig. 7a) although the extract of Co7.8, Co3.9 and Co0.78 films did show significant differences with it after 72 h of exposure (chronic toxicity) (Fig. 7d). Only the Co0 and Co0.078 extract samples showed no significant difference with respect to the control and the survival rate was more than 70%, indicating that the samples were not toxic. Body length was the second parameter analyzed to determine cobalt extract toxicity. Growth was measured by body length in a microscopic photo by Motic Images Plus 3.0 software. The data obtained were normalized considering the Control mean such as 100% of %Length. The results showed no significant difference between the Co0, Co7.8, Co3.9, Co0.78 and Co0.078 extracts and the control after 24 h (Fig. 7c) and 72 h (Fig. 7f) exposure. The last parameter analyzed to determine cobalt extract toxicity was reproduction, for which 3 nematodes were placed on a new plate and incubated for 48 h. The eggs were counted under a

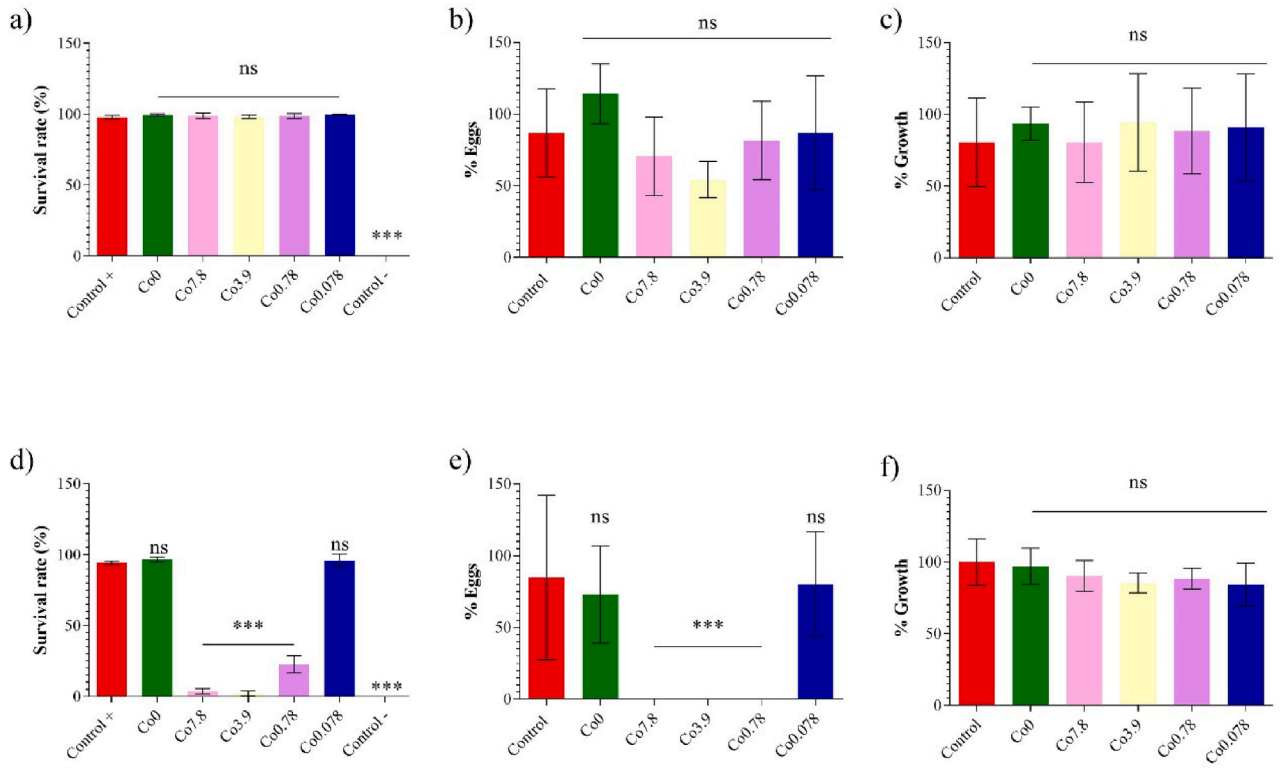

Fig. 7. Measured parameters of *Caenorhabditis elegans in vivo* toxicity to cobalt extracts after 24 h (acute toxicity) exposure: survival rate (a), reproduction (c) and body length (c); and after 72 h (chronic toxicity) exposure: survival rate (d), reproduction (e) and body length (f). Data are expressed as the mean ± standard deviation of six replicates (n = 6). The results of the statistical analysis with respect to positive control are indicated in the graph: *** p < 0.001, ns: not significant.

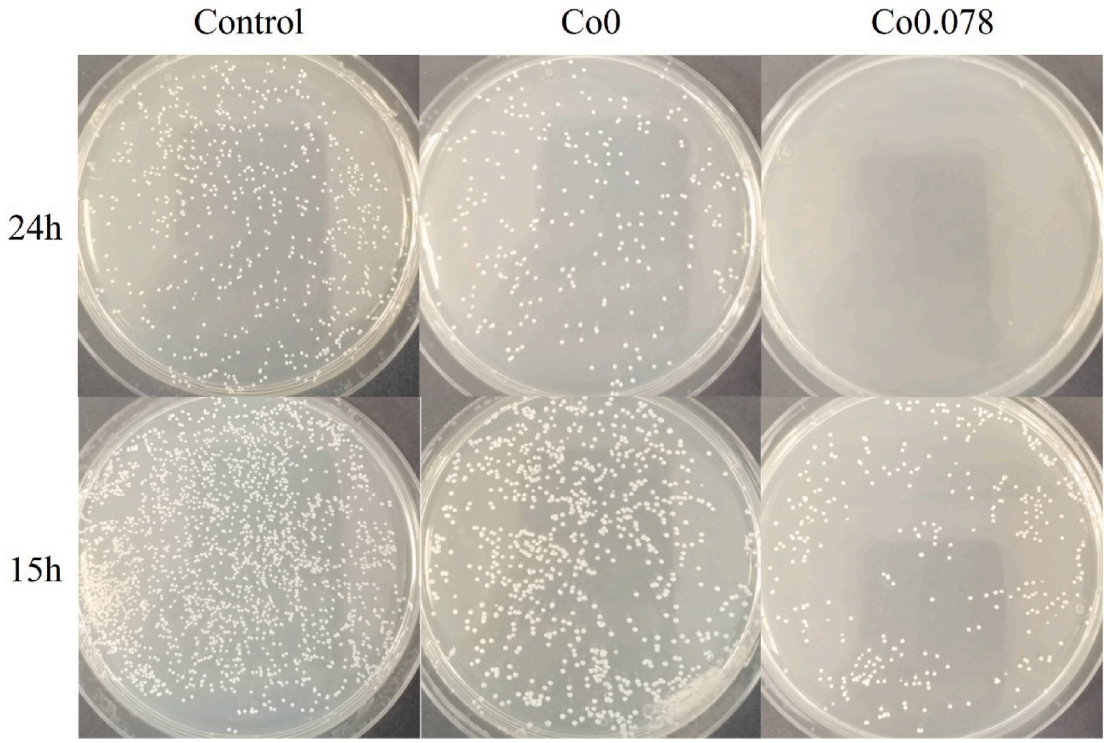

Fig. 8. Representative plate images with the Colony Forming Units (CFU) obtained in the antibacterial test of MRSA after 24 h and 15 h of exposure with a dilution factor of 10^{-6} with positive control, Co0 and Co0.078.

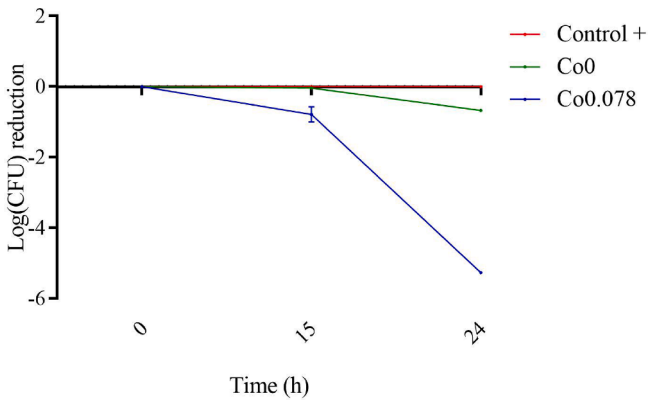

Fig. 9. CFU reduction in logarithm of plaque-forming units per mL (log(CFU/mL)). Control, untreated film (Co0), films treated with cobalt chloride (Co0.078) at 15 h and 24 h of bacterial contact with MRSA.

microscope, after which the data obtained were normalized considering the Control mean of 100% of %Eggs. After 24 h exposure (Fig. 7b), the results showed no significant difference between the cobalt extracts with respect to control. On the other hand, since the survival rate after 72 h exposure (Fig. 7e) was low in the Co7.8, Co3.9 and Co0.78 samples, they contained no eggs. Co0 and Co0.078 showed no significant difference with the control after 72 h exposure.

After analyzing these *in vitro* and *in vivo*, it was decided to carry out the following biological studies (antiviral, antibacterial and anticancer) only on the non-toxic samples (Co0 and Co0.078), which the only ones that can be used for biomedical applications.

3.7. Antibacterial activity

The antibacterial results of the positive control at 15 and 24 h of treated (Co0.078) and untreated (Co0) films against MRSA multidrug-resistant bacteria are shown in Fig. 8.

The results of the antibacterial activity showed that the Co0.078 film had antibacterial activity (Fig. 9) at 15 h and 24 h of bacterial contact with methicillin-resistant *Staphylococcus aureus* (MRSA), while, as expected, the positive control and the untreated film (Co0) showed no CFU reduction or antibacterial activity.

3.8. Anticancer study

Melanoma cells (B16) were treated with serial dilutions of the Co0 and Co0.078 extract samples for 24 h (Fig. 10a and 10b, respectively). Untreated film (Co0) showed no significant difference with the control, as expected. However, the undiluted Co0.078 extract did show significant differences with the control. Thus, cell viability of the Co0.078 extract was less than 50%.

Colon cancer cells (HT-29) were treated with serial dilutions of the extract of Co0 and Co0.078 samples for 24 h (Fig. 10c and 10d, respectively). Untreated film (Co0) showed no significant difference with the control, as expected. On the other hand, although the undiluted extract showed no significant differences with the control in the HT-29 cells, the diluted 1/10 of the extract of Co0.078 showed significant differences with the control. The cell viability of the Co0.078 WD is 76% and the cell viability of the Co0.01 10^{-1} was 66%. Although the graph shows a difference between the viability of both samples, the ANOVA with Tukey's post-hoc test shows no significant differences between the two samples.

3.9. Antiviral test using enveloped bacteriophage Φ6

The results of the antiviral tests showed that the cobalt film (Co0.078) possesses antiviral activity at 24 h of viral contact with the bacteriophage Φ6 (Fig. 11).

Thus, after 24 h of contact between the cobalt film (Co0.078) and the SARS-CoV-2 viral model, bacterial lawns grew in the plate with few plaques (Fig. 11). On the other hand, the untreated film (Co0) showed

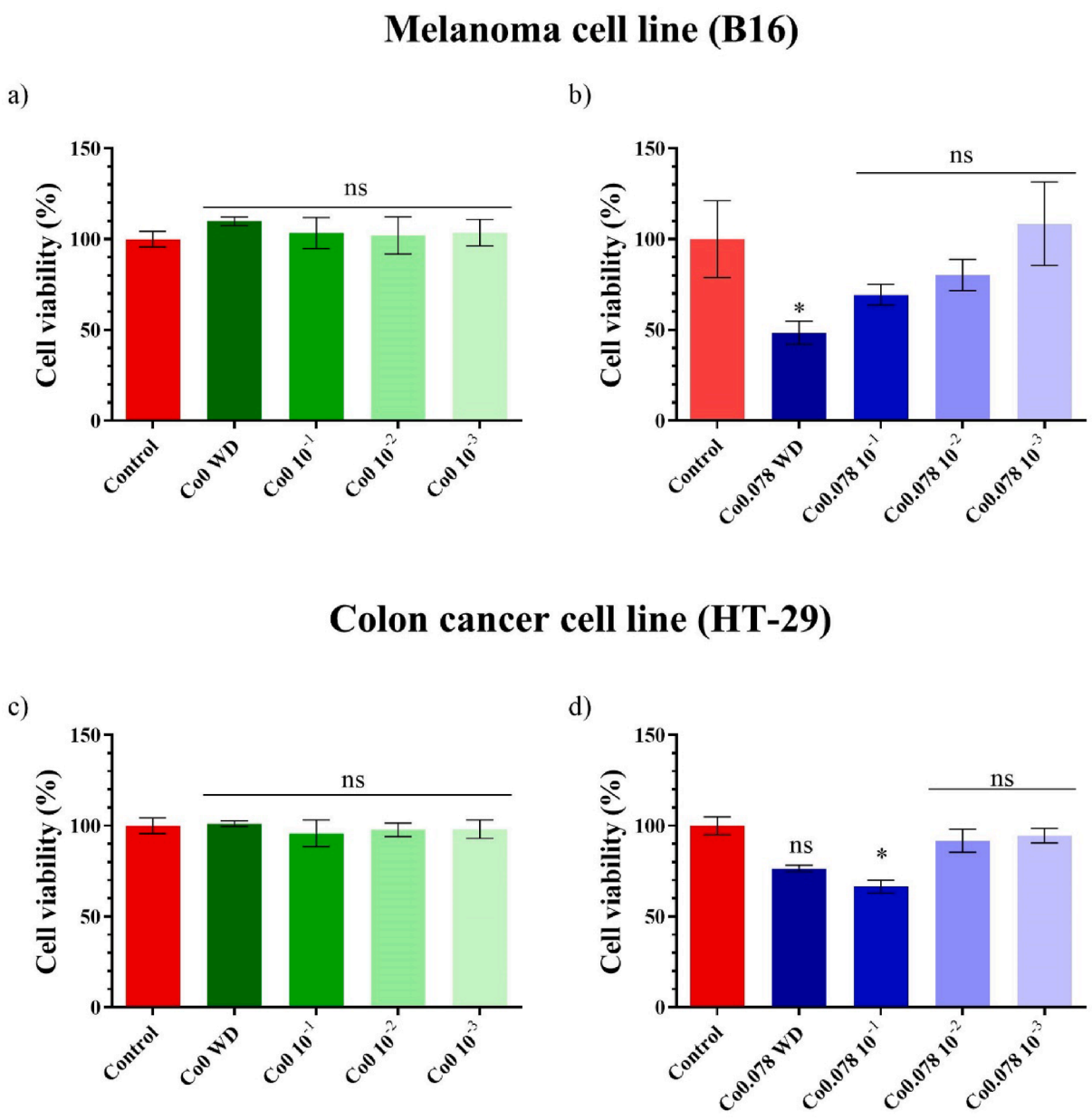

Fig. 10. Anticancer activity of extracts of the Co0 (a) and Co0.078 (b) films in melanoma (B16) for 24 h of exposure and anticancer activity of extracts of the Co0 (c) and Co0.078 (d) films in colon cancer cells (HT-29) for 24 h of exposure. The results of the extracts are shown for undiluted (WD) and diluted at 10^{-1}, 10^{-2} and 10^{-3}. Data are expressed as the mean ± standard deviation of six replicates. The results of the statistical analysis with respect to control are indicated in the graph: * $p < 0.1$; ns: not significant.

the same behaviour than Co0.078. The plaque-forming units per mL (PFU/mL) of bacteriophage Φ6 after being in contact with the Co0 and Co0.078 is shown and compared with the control in Fig. 12.

The antiviral activity of alginate crosslinked with calcium was demonstrated in a previous publication [3]. Therefore, the Co0.078 film keeps the antiviral activity of calcium alginate because the % inactivation of the virus is close to 100% in both samples (Table 2).

The *in vivo* and *in vitro* biocompatible Co0.078 film crosslinked with Ca^{2+} and Co^{2+} manifests antiviral, antibacterial and anticancer activity. Although the antimicrobial mechanism of cobalt is still not fully elucidated,[32] the antimicrobial and anticancer mechanism of action of Co^{2+} against bacterial, viral phospholipid membranes and cancer cells must be related to its positive charge and electronegativity (1.91) similar to those of other well-known antimicrobial and anticancer cations such as copper and silver (1.90 and 1.93, respectively).

Therefore, these new biofunctional alginate-based hydrogels are very promising for biomedical applications. However, more research is necessary in order to demonstrate whether the hydrogel would have any adverse effects when used *in vivo* or whether the observed biological properties would persist over time.

4. Conclusions

Novel alginate films crosslinked with Ca^{2+} and different amounts of Co^{2+} ions were prepared by the solvent casting method. The hydrogel with the fewest cobalt ions was biocompatible in keratinocyte cells and also *in vivo*, using the *C. elegans* model. This hydrogel showed antibacterial activity against the MRSA multidrug-resistant bacteria and antiviral activity (98.01% viral inactivation) against a surrogate of SARS-CoV-2 and other enveloped viruses, including influenza and Ebola. This advanced biocompatible hydrogel film showed a slow degradation behavior in acid aqueous medium and anticancer properties against

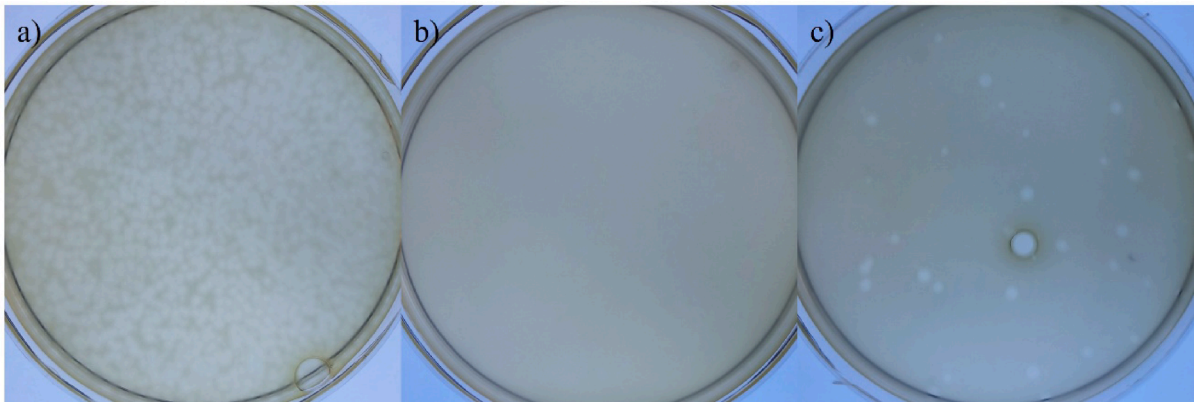

Fig. 11. Loss of bacteriophage phi 6 viability measured by the double-layer method. Bacteriophage phi 6 titration images of 1/10 diluted samples for control (a), untreated film (Co0) (b), film treated by cobalt (Co0.078) (c) at 24 h of viral contact.

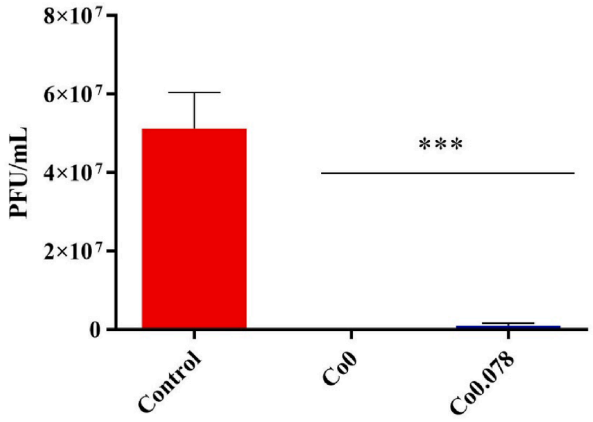

Fig. 12. Reduction of infection titers of the phi 6 bacteriophage in plaque-forming units per mL ((PFU/mL)) measured by the double-layer method. Control, untreated film (Co0), film treated with cobalt (Co0.078) at 24 h of viral contact. The results of the statistical analysis with respect to control are indicated in the graph: *** $p > 0.001$.

Table 2
Infection titers obtained by the double-layer method for the antiviral assay performed with bacteriophage Φ6 expressed as mean ± standard deviation, percentage of viral inactivation and log(PFU/mL) reduction with respect to Control and after being in contact with the untreated film (Co0), and the cobalt (Co0.078) for 24 h of viral contact.

	Control	Co0	Co0.078
PFU/mL	$5.12 \times 10^7 \pm 9.23 \times 10^6$	0.00 ± 0.00	$1.02 \times 10^6 \pm 6.63 \times 10^5$
log reduction	–	7.70	1.75
% inactivation virus	–	100	98.01

melanoma and colon cancer cells. These promising results indicate that further research should be carried out in this area towards new biomedical applications for the novel alginate-based hydrogel film developed in the current work.

CRediT authorship contribution statement

Alba Cano-Vicent: Supervision, Writing – review & editing, Writing – original draft, Visualization, Resources, Investigation, Software, Formal analysis. **Andrea Martínez-Agut:** Resources. **Alberto Tuñón-Molina:** Resources. **Hamid Bakshi:** Project administration, Resources, Software, Formal analysis. **Roser Sabater i Serra:** Supervision, Writing – original draft, Visualization, Data curation, Resources, Investigation, Software, Formal analysis. **Iman M. Alfagih:** Resources. **Murtaza M. Tambuwala:** Project administration, Supervision, Data curation, Resources, Software, Formal analysis. **Ángel Serrano-Aroca:** Funding acquisition, Project administration, Supervision, Writing – review & editing, Writing – original draft, Visualization, Data curation, Resources, Investigation, Software, Formal analysis, Conceptualization, Methodology, Validation.

Declaration of Competing Interest

The authors declare that they have no known competing financial interests or personal relationships that could have appeared to influence the work reported in this paper.

Data availability

Data will be made available on request.

Acknowledgments

The authors would like to express their gratitude to the Fundación Universidad Católica de Valencia San Vicente Mártir and to the Spanish Ministry of Science and Innovation for their financial support through Grant 2020-231-006UCV and PID2020-119333RB-I00 / AEI / 10.13039/501100011033, respectively. TheCIBER-BBNinitiativeis funded by the VI National R&D&I Plan 2008 – 2011, Iniciativa Ingenio 2010, Consolider Program.CIBER actions are financed by the Instituto de Salud CarlosIII with assistance from the European Regional Development. Funding support also from Researchers Supporting Project number (RSP-2023R782), King Saud University, Riyadh, Saudi Arabia.

References

[1] E.M. Ahmed, Hydrogel: Preparation, characterization, and applications: A review, J. Adv. Res. 6 (2015) 105–121, https://doi.org/10.1016/J.JARE.2013.07.006.
[2] E. R. Banerjee, ed., Nanomaterials and Biomedicine: Therapeutic and Diagnostic Approach, (2020). Springer Nature, Singapore, 2020. https://doi.org/10.1007/978-981-15-5274-8.
[3] A. Cano-Vicent, R. Hashimoto, K. Takayama, Á. Serrano-Aroca, Biocompatible Films of Calcium Alginate Inactivate Enveloped Viruses Such as SARS-CoV-2, Polymers (Basel). 14 (2022) 1483, https://doi.org/10.3390/POLYM14071483.
[4] A. Zheng, L. Cao, Y. Liu, J. Wu, D. Zeng, L. Hu, X. Zhang, X. Jiang, Biocompatible silk/calcium silicate/sodium alginate composite scaffolds for bone tissue engineering, Carbohydr. Polym. 199 (2018) 244–255, https://doi.org/10.1016/J.CARBPOL.2018.06.093.
[5] C. Lee, J. Shin, J.S. Lee, E. Byun, J.H. Ryu, S.H. Um, D.I. Kim, H. Lee, S.W. Cho, Bioinspired, calcium-free alginate hydrogels with tunable physical and mechanical properties and improved biocompatibility, Biomacromolecules 14 (2013)

2004–2013, https://doi.org/10.1021/BM400352D/ASSET/IMAGES/LARGE/BM-2013-00352D_0008.JPEG.
[6] E.A. Nunamaker, E.K. Purcell, D.R. Kipke, In vivo stability and biocompatibility of implanted calcium alginate disks, J. Biomed. Mater. Res. A 83A (2007) 1128–1137, https://doi.org/10.1002/JBM.A.31275.
[7] A. Hurtado, A.A.A. Aljabali, V. Mishra, M.M. Tambuwala, Á. Serrano-Aroca, Alginate: Enhancement Strategies for Advanced Applications, Int. J. Mol. Sci., 2022, Vol. 23, Page 4486. 23 (2022) 4486. https://doi.org/10.3390/IJMS23094486.
[8] H.T.P. Anh, C.M. Huang, C.J. Huang, Intelligent Metal-Phenolic Metallogels as Dressings for Infected Wounds, Sci. Rep. 9 (2019) 1–10, https://doi.org/10.1038/s41598-019-47978-9.
[9] M. Shahriari-Khalaji, S. Hong, G. Hu, Y. Ji, F.F. Hong, Bacterial Nanocellulose-Enhanced Alginate Double-Network Hydrogels Cross-Linked with Six Metal Cations for Antibacterial Wound Dressing, Polymers 2020, Vol. 12, Page 2683. 12 (2020) 2683. https://doi.org/10.3390/POLYM12112683.
[10] R. Jahanban-Esfahlan, H. Derakhshankhah, B. Haghshenas, B. Massoumi, M. Abbasian, M. Jaymand, A bio-inspired magnetic natural hydrogel containing gelatin and alginate as a drug delivery system for cancer chemotherapy, Int. J. Biol. Macromol. 156 (2020) 438–445, https://doi.org/10.1016/J.IJBIOMAC.2020.04.074.
[11] P. Tan, X. Chen, H. Zhang, Q. Wei, K. Luo, Semin. Cancer Biol. 89 (2023) 61–75, https://doi.org/10.1016/j.semcancer.2023.01.005.
[12] H. Li, J. Sun, H. Zhu, H. Wu, H. Zhang, Z. Gu, K. Luo, Recent advances in development of dendritic polymer-based nanomedicines for cancer diagnosis, Wiley Interdiscip. Rev. Nanomed. Nanobiotechnol. 13 (2021) e1670.
[13] A.M. El-Kady, A.A. Ali, A. El-Fiqi, Controlled delivery of therapeutic ions and antibiotic drug of novel alginate-agarose matrix incorporating selenium-modified borosilicate glass designed for chronic wound healing, J. Non Cryst. Solids 534 (2020), 119889, https://doi.org/10.1016/J.JNONCRYSOL.2020.119889.
[14] A.I. Rezk, F.O. Obiweluozor, G. Choukrani, C.H. Park, C.S. Kim, Drug release and kinetic models of anticancer drug (BTZ) from a pH-responsive alginate polydopamine hydrogel: Towards cancer chemotherapy, Int. J. Biol. Macromol. 141 (2019) 388–400, https://doi.org/10.1016/J.IJBIOMAC.2019.09.013.
[15] B. Frígols, M. Martí, B. Salesa, C. Hernández-Oliver, O. Aarstad, A.-S.-T. Ulset, G. I. Sætrom, F.L. Aachmann, Á. Serrano-Aroca, Graphene oxide in zinc alginate films: Antibacterial activity, cytotoxicity, zinc release, water sorption/diffusion, wettability and opacity, PLoS One 14 (2019), https://doi.org/10.1371/journal.pone.0212819.
[16] S.R. Gill, D.E. Fouts, G.L. Archer, E.F. Mongodin, R.T. DeBoy, J. Ravel, I.T. Paulsen, J.F. Kolonay, L. Brinkac, M. Beanan, R.J. Dodson, S.C. Daugherty, R. Madupu, S. V. Angiuoli, A.S. Durkin, D.H. Haft, J. Vamathevan, H. Khouri, T. Utterback, C. Lee, G. Dimitrov, L. Jiang, H. Qin, J. Weidman, K. Tran, K. Kang, I.R. Hance, K. E. Nelson, C.M. Fraser, Insights on evolution of virulence and resistance from the complete genome analysis of an early methicillin-resistant Staphylococcus aureus strain and a biofilm-producing methicillin-resistant Staphylococcus epidermidis strain, J. Bacteriol. 187 (2005) 2426–2438, https://doi.org/10.1128/JB.187.7.2426-2438.2005.
[17] F.L. Hakkim, H.A. Bakshi, S. Khan, M. Nasef, R. Farzand, S. Sam, L. Rashan, M. S. Al-Baloshi, S.S.A.A. Hasson, A. al Jabri, P.A. McCarron, M.M. Tambuwala, Frankincense essential oil suppresses melanoma cancer through down regulation of Bcl-2/Bax cascade signaling and ameliorates heptotoxicity via phase I and II drug metabolizing enzymes, Oncotarget 10 (2019) 3472–3490. https://doi.org/10.18632/oncotarget.26930.
[18] R. el Haidari, L.A. Abbas, V. Nerich, A. Anota, Factors associated with health-related quality of life in women with breast cancer in the middle east: A systematic review, Cancers (Basel). 12 (2020) 696, https://doi.org/10.3390/cancers12030696.
[19] H.A. Bakshi, G.A. Quinn, M.M. Nasef, V. Mishra, A.A.A. Aljabali, M. El-Tanani, Á. Serrano-Aroca, M.W. da Silva, P.A. McCarron, M.M. Tambuwala, Crocin Inhibits Angiogenesis and Metastasis in Colon Cancer via TNF-α/NF-kB/VEGF Pathways, Cells. 11 (2022) 1502, https://doi.org/10.3390/cells11091502.
[20] A.M. Kropinski, A. Mazzocco, T.E. Waddell, E. Lingohr, R.P. Johnson, Enumeration of bacteriophages by double agar overlay plaque assay, Methods Mol. Biol. 501 (2009) 69–76, https://doi.org/10.1007/978-1-60327-164-6_7.
[21] J.T.N. Knijnenburg, P. Kasemsiri, K. Amornrantanaworn, S. Suwanree, W. Iamamornphan, P. Chindaprasirt, K. Jetsrisuparb, Entrapment of nano-ZnO into alginate/polyvinyl alcohol beads with different crosslinking ions for fertilizer applications, Int. J. Biol. Macromol. 181 (2021) 349–356, https://doi.org/10.1016/J.IJBIOMAC.2021.03.138.
[22] L. Fuks, D. Filipiuk, M. Majdan, Transition metal complexes with alginate biosorbent, J. Mol. Struct. 792–793 (2006) 104–109, https://doi.org/10.1016/J.MOLSTRUC.2005.12.053.
[23] E. Fourest, B. Volesky, Alginate Properties and Heavy Metal Biosorption by Marine Algae, Appl. Biochem. Biotechnol. - Part A Enzyme Eng. Biotechnol. 67 (1997) 215–226, https://doi.org/10.1007/BF02788799.
[24] I. Braccini, S. Pérez, Molecular Basis of Ca2+-Induced Gelation in Alginates and Pectins: The Egg-Box Model Revisited, Biomacromolecules 2 (2001) 1089–1096, https://doi.org/10.1021/BM010008G.
[25] L. Gonzalez-Moragas, A. Roig, A. Laromaine, C. elegans as a tool for in vivo nanoparticle assessment, Adv. Colloid Interface Sci. 219 (2015) 10–26, https://doi.org/10.1016/J.CIS.2015.02.001.
[26] P.E. Kuwabara, N. O'Neil, The use of functional genomics in C. elegans for studying human development and disease, J. Inherit. Metab. Dis. 24 (2001) 127–138, https://doi.org/10.1023/A:1010306731764.
[27] E.L.L. Sonnhammer, R. Durbin, Analysis of Protein Domain Families inCaenorhabditis elegans, Genomics 46 (1997) 200–216, https://doi.org/10.1006/GENO.1997.4989.
[28] V.M. Chauhan, G. Orsi, A. Brown, D.I. Pritchard, J.W. Aylott, Mapping the pharyngeal and intestinal pH of Caenorhabditis elegans and real-time luminal pH oscillations using extended dynamic range pH-sensitive nanosensors, ACS Nano 7 (2013) 5577–5587, https://doi.org/10.1021/NN401856U.
[29] K. Stutz, A. Kaech, M. Aebi, M. Künzler, M.O. Hengartner, Disruption of the C. elegans Intestinal Brush Border by the Fungal Lectin CCL2 Phenocopies Dietary Lectin Toxicity in Mammals, PLoS One. 10 (2015). https://doi.org/10.1371/JOURNAL.PONE.0129381.
[30] Y. Zhang, X. Zou, Y. Ding, H. Wang, X. Wu, B. Liang, Comparative genomics and functional study of lipid metabolic genes in Caenorhabditis elegans, BMC Genomics 14 (2013) 164, https://doi.org/10.1186/1471-2164-14-164.
[31] P.R. Hunt, The C. elegans model in toxicity testing, J. Appl. Toxicol. 37 (2017) 50, https://doi.org/10.1002/JAT.3357.
[32] E.M. Cazalini, W. Miyakawa, G.R. Teodoro, A.S.S. Sobrinho, J.E. Matieli, M. Massi, C.Y. Koga-Ito, Antimicrobial and anti-biofilm properties of polypropylene meshes coated with metal-containing DLC thin films, J. Mater. Sci. - Mater. Med. 28 (2017) 1–10, https://doi.org/10.1007/s10856-017-5910-y.